EE191 (Project Based Learning)

BALL POSISTION CONTROL ON A TILTING BALANCE BEAM

Group 2 :
Group Member Names -
Padhraic Barnes, Christian Botezatu, Aidan Doherty, Cian Farrell, Eoghan Farrelly, Ameen Hacini, Thomas Stack, Krystian Stratynski, Sarah Wang

Project Facilitator: Bob Lawlor

09/05/2025

Department of Electronic Engineering
Maynooth University

ABSTRACT

This project was about designing a feedback control system to move and balance a ball on a beam using a PID controller. We built a setup where a ball rolls along a beam, and the beam tilts based on input from an ultrasonic sensor that tracks the ball's position. The beam is moved by a servo motor, which is controlled using a Simulink model and a tuned PID system. The main goal was to get the ball to move to the centre of the beam and stay there, even if disturbed. This project is important because it applies core principles of control systems, mechanics, and programming in a hands-on way. The same type of system is used in real-world technologies like robotics, self-balancing systems (like Segways), and industrial automation where precision and feedback control are key. By working on this, we learned how to model a physical system, apply theory to practice, and test and refine a control loop in a realistic setting. It's a simple but powerful example of how engineers design systems that can react to their environment and maintain stability.

Contents

1 INTRODUCTION

This project focuses on designing a closed loop feedback control system to balance a ball on a beam by adjusting the beam's angle using a servo motor. A PID controller was used to process real-time data from an ultrasonic sensor, allowing the system to stabilize the ball at a target position. This kind of setup is a classic example in control systems engineering that we learn about in our EE114 module, commonly used to demonstrate principles of feedback, stability, and system response [8].

For our project, the ball and beam system is naturally unstable and requires constant feedback to maintain balance [7]. PID controllers are often used due to their simplicity and effectiveness in managing such dynamic systems. More advanced approaches, like state-space control, have also been explored, but PID remains popular for its ease of implementation and tuning.

2 LITERATURE REVIEW

Starting this project, the group had limited knowledge on the subject being delt with outside of the theory taught during EE114 System and Control which provided a base level of understanding regarding feedback control loops [8]. To better explore the specific problems related to PID control while dealing with balance beam related projects, many papers detailing similar projects completed by peers in similar studies were reviewed to explore different approaches to engineering our solution. Three papers provided particularly useful insight into both solution approaches and challenges to avoid as well a reference points to refer to as we made progress throughout the project. These papers were titled and referenced below as:

1.” Balancing a ball and beam with PID” [1]

2.“Ball Balancing Beam Design of a PID-controller” [6]

3.“Design and Implementation a Ball Balancing System for Control Theory” [7]

Throughout all three of these papers many similarities were apparent, most notably though were the control objective – to stabilise a ball on a naturally unstable beam system, using mathematical modelling to describe the system behaviour specifically based on Newtonian mechanics and using a PID controller as the primary control method to stabilise the system. When approaching the project, it was realised that all the above applied to our own system.

Regarding the mathematical modelling in particular, paper 1 was especially insightful, offering a frame of reference for how to approach the modelling using our own mathematical methods.
The main difference found in this was the method of transformation used, in which paper 1 describes a mathematical modelling process that the group was not familiar with. Feeling that it was overcomplicated for what we needed to do, this method was sidelined as an alternative to consider.
All reports offered an overview on the many issues to consider and avoid when working towards the solution, from design flaws to the effect of outside disturbance on hardware outputs.

Paper 2 contained similar information to paper 1. The paper elaborated on the algorithm used to design the PID controller and the standard representation of the PID controller in a manner that was more understandable to us. It also provided us with awareness of aspects to consider while implementing PID controller in practice. The paper did aid us in terms of learning about PID while advancing deeper into the PID process, further than was necessary for us to explore.

Paper 3 breaks down the physical system design and is very informative which gave us useful intuition on our project. The paper effectively details what to do and what not to do in terms of building a

working model of a ball-balancing beam to represent our mathematical equations. It aided us with things like solutions on materials to use, location and stability of the motor, along with what to avoid in both sections such as instable mounting etc. The paper also recommended the use of MATLAB to model the response of our system equations.

3 PROPOSED APPROACH

The aim of the project involves creating a feedback control system to move a ball on an articulating balance beam to a desired setpoint along the beam and keep it there. To approach this, the team proposed building a beam with an ultrasonic sensor mounted to one end, controlled by a servo which receives input to tilt the beam to direct a ball to the desired position (setpoint). Proposed build model pictured below [Figure 1]:

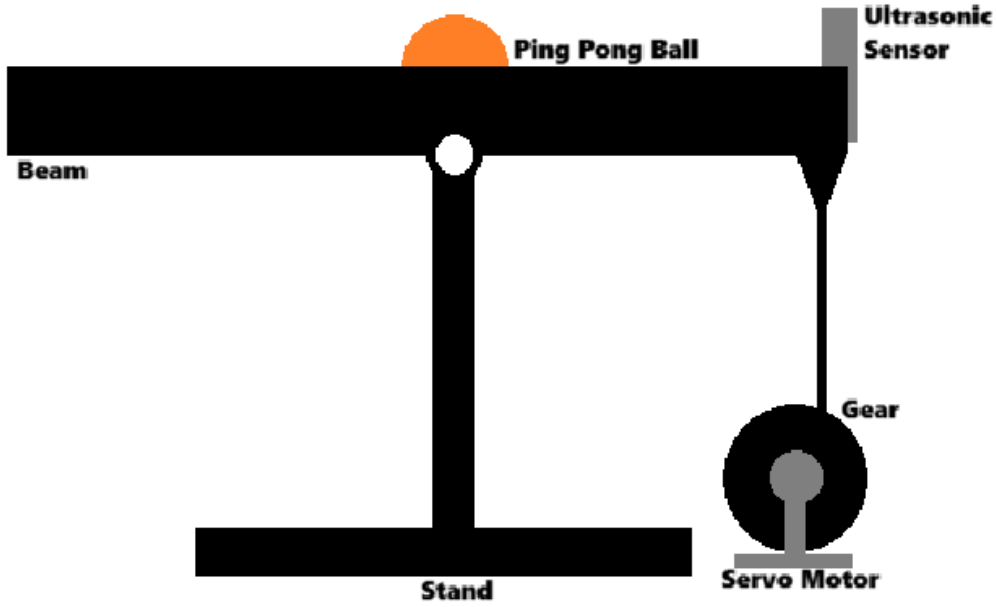

Figure 1: Diagram of Proposed Build

The PID control system will receive continuous input from the ultrasonic sensor, marking the position of the ball and output an angle at which to tilt the motor shaft. The desired output is set to the centre point of the beam, a certain distance away from the sensor, considering an error of ± 0.01 metres. Proposed control system pictured below [Figure 2]:

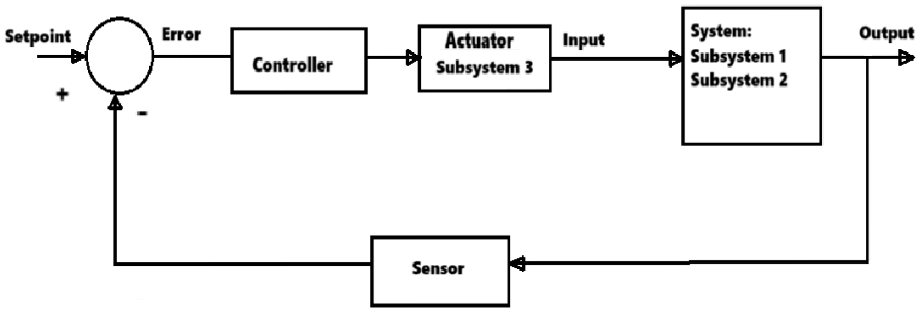

Figure 2: Diagram of Feedback Loop

3.1 Mathematical Theory

3.1.1 Ball motion on angled beam.

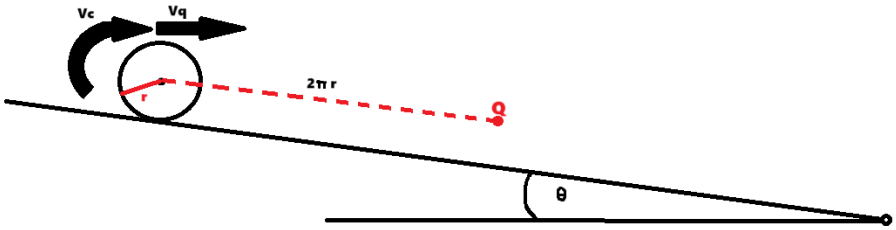

Figure 3: Diagram of Ball Motion

'Pure roll'/ 'rolling without slipping' is described as when a sphere with centre 'Q' and radius 'r' has made a complete rotation with the point 'Q' having moved over a distance of 2πr meters [3]. When 'pure roll' occurs, the velocity of the point 'Q' equals the velocity of the circumference of the sphere. When a sphere of mass 'm' is placed on a slope of angle 'θ' to the horizontal, the following forces are present:

Reference for equations: [4]

F = ma, where 'm' is mass in Kg, 'a' is acceleration in ms^{-2} and 'F' is force in Newtons

Equation 1: Total Force

$$F_{total} = mgsin\theta - F_r$$

Equation 1 where θ is the angle of the slope in radians, 'F_r' is the friction force in Newtons, and 'g' is acceleration due to gravity in ms^{-2}

Friction can be totalled to = $\frac{I_q a}{r^2}$, where I_q is the inertia and 'r' is the radius of the sphere in meters [4], leaving Equation 2

Equation 2: Force Equation Considering Inertia

$$F_{total} = mgsin\theta - \frac{I_q a}{r^2}$$

Inertia of a hollow sphere:

Equation 3: Inertia

$$I_q = \frac{2}{3}mr^2 \text{ [3]}$$

Substituting all values into the equation gives:

Equation 4: Force Equation

$$ma = mgsin\theta - \frac{\frac{2}{3}mr^2 a}{r^2}$$

Solving for the value of 'a' leaves Equation 4 considering that 'a' is the double derivative of displacement (d), a = $\ddot{x}$

Equation 5: Acceleration of Ball with Respect to Angular Displacement

$$a = \frac{3}{5} g sin\theta$$

$$\ddot{x} = \frac{3}{5} g sin\theta$$

The initial equation taken from the theory

, where:

$\ddot{x}$=Second derivative of displacement (acceleration)

g= gravity

Θ= angular displacement

I= Inertia of a hollow sphere

Equation 6: Complete Differential

$$\ddot{x} = \frac{3}{5} g sin\Theta$$

This second-order differential equation must be converted into an algebraic equation to make it easier to solve. To do this, the Laplace transform must be implemented [9].

Equation 7: Laplace Transform

$$L\{\ddot{x}(t)\} = s^2X(s) - sx(0) - \dot{x}(0)$$

Equation 8: Laplace Transform

$$L\{\frac{3}{5}\,\theta(t)\} = \frac{3}{5} g.\Theta(s)$$

Equation 9: Putting Both Sides Together

$$s^2X(s) - sx(0) - \dot{x}(0) = \frac{3}{5} g.\Theta(s)$$

To implement this system into Simulink and run testing, it must be converted into a transfer function [10].

Equation 10: Taking Laplace transform of both sides

$$s^2X(s) = \frac{3}{5} g\Theta(s)$$

$$=> X(s) = \frac{3}{5} . \frac{g}{s^2} . \Theta(s)$$

Equation 11: Rearranging equation 10 for the transfer function

$$H(s) = \frac{X(s)}{\Theta(s)}$$

$$=> H(s) = \frac{\frac{3}{5} . \frac{g}{s^2} . \Theta(s)}{\Theta(s)}$$

$$=> H(s) = \frac{3}{5} . \frac{g}{s^2}$$

Final Transfer function:

$$H(s) = \frac{3g}{5s^2}$$

Implementing this into Simulink [8]:

g must be set to 9.81 in the Matlab command window first.

3.1.2 Subsystem 2 – Mechanical Linkage

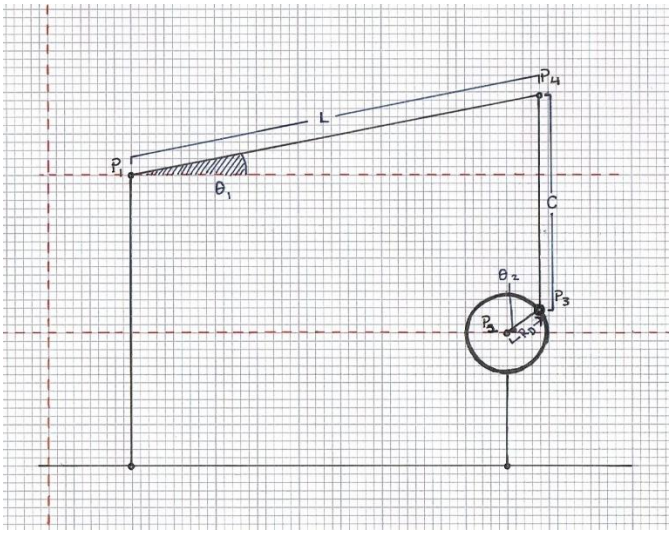

Figure 4: Mechanical Linkage Diagram

Table 1: Mechanical Linkage Algebraic Terms

Symbol	Description	SI Unit(s)
P_1	Fixed point about which L can rotate freely.	m (Metre)
θ_1	Angle between L and the positive horizontal axis. (Output of the system)	rad (radians)
L	Length of the arm from the fixed point P_1 to the moving point P_3.	m (Metre)
P_3	Moving point at the centre of rotation about which C and L rotate.	m (Metre)
C	Length of the connecting rod between P_3 and P_4. Connection points to L and C can rotate freely.	m (Metre)
P_4	Moving point at the centre of rotation about which C and R rotate.	m (Metre)
R_D	Length of the arm from the motor shaft P_2 to the moving point P_4.	m (Metre)
θ_2	Angle between R and the positive horizontal axis. (Input to the system)	rad (radians)
P_2	Position of the motor shaft that controls the rotation of R.	m (Metre)

System Assumptions:

- No movement in the z-axis.
- All parts of the assembly are rigid apart from the rotational points.

The system input(θ_2) is the angular position of the motor disk, the system output(θ_1) in the angular position of the beam, both relative to the horizontal axis. The relationship between θ_1 and θ_2 can be solved for by relating the points P_3 and P_4 using the distance between two points formula. Rearranging for Sin(θ_1) results in a 2^{nd} order polynomial (Equation 12).

Equation 12: Distance Between Points P_4 and P_3 Rearranged for Sin(θ_1).

$$C^2 = (P_{4y} - P_{3y})^2 + (P_{4x} - P_{3x})^2$$

$$=> C^2 = (P_{1y} + Lsin(\theta_1) - (P_{2y} + R_D sin(\theta_2)))^2 + (P_{1x} + Lcos(\theta_1) - (P_{2x} + R_D cos(\theta_2)))^2$$

$$=>$$

$$(2L)^2\left(\left(P_{1y} - P_{2y} - R_D sin(\theta_2)\right)^2 + \left(P_{1x} - P_{2x} - R_D cos(\theta_2)\right)^2\right)(sin\theta_1)^2 + (4L)\left(P_{1y} - P_{2y} - R_D sin(\theta_2)\right)\left(R_D^2 + L^2 + \left(P_{1y} - P_{2y}\right)^2 + (P_{1x} - P_{2x})^2 - C^2 + (2R_D)\left(\left(-P_{1y} + P_{2y}\right)\sin(\theta_2) + (-P_{1x} + P_{2x})\cos(\theta_2)\right)\right)(sin\theta_1) + \left(R_D^2 + \left(P_{1y} - P_{2y}\right)^2 + (P_{1x} - P_{2x})^2 - C^2 + (2R_D)\left(\left(-P_{1y} + P_{2y}\right)\sin(\theta_2) + (-P_{1x} + P_{2x})\cos(\theta_2)\right)\right)^2 + (L^2)\left(L^2 + 2\left(R_D^2 + \left(P_{1y} - P_{2y}\right)^2 + (P_{1x} - P_{2x})^2 - C^2 + (2R_D)\left(\left(-P_{1y} + P_{2y}\right)\sin(\theta_2) + (-P_{1x} + P_{2x})\cos(\theta_2)\right)\right)\right) - \left((2L)\left(P_{1x} - P_{2x} - R_D cos(\theta_2)\right)\right)^2 = 0$$

Using the minus b formula on Equation 12 yields the two real values for Sin(θ_1) if they exist for a given set of parameters. Applying the arcsine function yields θ_1 (Equation 13).

Equation 13: Minus b Formula (Only + Version Used for this Application)

$$sin(\theta_1) = \frac{-b + \sqrt{b^2 - 4ac}}{2a}$$

$$=> \theta_1 = \arcsin\left(\frac{-b + \sqrt{b^2 - 4ac}}{2a}\right)$$

Once Equation 13 is evaluated, the result will be compared to the partial linear approximation (Equation 14) of the system found in the literature review, to determine a range of motion that allows the system to operate without excessive error.

Equation 14: Partial Linear Approximation of Equation 2

$$Lsin(\theta_1) = R_D sin(\theta_2)$$

$$=> \theta_1 = \arcsin\left(\frac{R_D}{L}\sin(\theta_2)\right)$$

This may then be further simplified to a fully linear form (Equation 15). Note performing this step requires that θ_2 be kept as small as possible as the error in this assumption increases as it moves from 0 to ±90°.

Equation 15: Linear Approximation of Equation 3

$$L\theta_1(t) = R_D\theta_2(t)$$

$$=> \theta_1(t) = \frac{R_D}{L}\theta_2(t)$$

$$=> L\left\{\theta_1(t) = \frac{R_D}{L}\theta_2(t)\right\}$$

$$=> \theta_1(s) = \frac{R_D}{L}\theta_2(s)$$

$$\frac{\theta_1(s)}{\theta_2(s)} = \frac{R_D}{L}$$

3.1.3 Subsystem 3 – DC servo position control

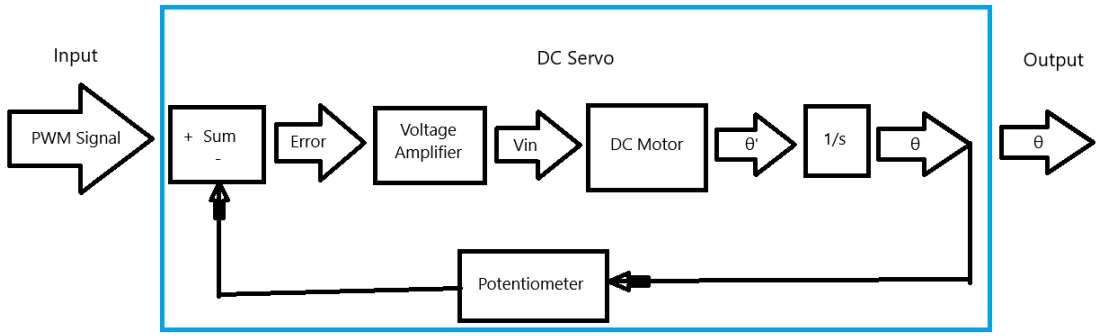

Figure 5: Servo Block Diagram

A servo is a specific type of motor assembly that has a potentiometer attached to its output shaft, the resistance of the potentiometer changes based on the shaft's rotational position. This allows for an input PWM voltage to be compared to the voltage through the potentiometer to generate an error signal. This error is then passed through a voltage amplifier to multiply the error by some constant value and outputs a voltage that is then fed into the internal DC motor. The voltage amplifier acts as a proportional controller. Based on the applied voltage, the motor accelerates the output shaft towards the desired setpoint dictated by the PWM input until the error is eliminated.

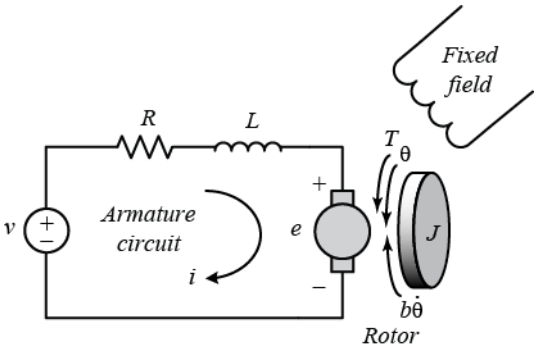

Figure 6: DC Motor Electrical Circuit (left) and Mechanical Force Diagram (right) [12]

Examining the workings of a DC motor yields two differential equations, one based on the mechanical forces (Equation 16) and one based on the electrical circuit (Equation 17). Given the limitations of the team's experience Equation 17 will be simplified by assuming the value of the inductor 'L' is zero. These equations can be related using the torque constant of the motor (Equation 18) and the back emf constant (Equation 19). Substituting in these constants yields Equation 20 and Equation 21, then substituting Equation 20 into Equation 21 yields the motor's differential equation. Finally, we take the Laplace transform of Equation 21 and rearrange for the transfer function, with voltage applied to the motor($v_{in}(s)$) as the input and the angular velocity($s\theta(s)$) as the output.

Table 2: DC Motor Algebraic Terms

Symbol	Description	SI Unit(s)
θ``	Angular acceleration of the motor shaft.	rad/s^2 (Radians per second^2)
θ`	Angular velocity of the motor shaft. (System output)	rad/s (Radians per second)
J	Moment of inertia of the motor shaft, plus the load attached to the shaft.	Kgm^2 (Kilogram metre^2)
T_m	Torque developed by the motor.	Nm (Newton metre)
b	Friction constant of the motor.	Nm/(rad/s) (Newton metre per radians per second)
i	Current passing through the motor circuit.	A (Ampere)
R	Resistance of the wire within the motor.	Ω (Ohm)
L	Inductance of the motor coil.	H (Henry)
v_{EMF}	Voltage generated by the motor coil spinning within the magnetic field.	V (Volt)
v_{in}	Voltage applied to the motor. (System Input)	V (Volt)
K_T	Torque constant of the motor. (Equal to K_b if both are in SI units)	Nm/A (Newton metre per Amp)
K_b	Back EMF constant of the motor. (Equal to K_T if both are in SI units)	V/(rad/s) (volts per radians per second)

Reference source for equations: [13]

Equation 16: Motor Mechanical Forces

$$J\theta'' = T_m - b\theta'$$

Equation 17: Kirchoff's Voltage Law applied to DC Motor Circuit (V_{EMF} = e from Figure 6)

$$v_{in} = iR + Li' + v_{EMF} \approx iR + v_{EMF}$$

$$v_{in} \approx iR + v_{EMF}$$

Equation 18: Motor Torque Constant

$$K_T = \frac{T_m}{i}$$

$$=> \ T_m = K_T i$$

Equation 19: Back emf Constant

$$K_b = \frac{v_{EMF}}{\theta'}$$

$$=> \ v_{EMF} = K_b \theta'$$

Equation 20: Substituting Equation 7 into Equation 5 and rearranging for 'i'

$$J\theta'' = K_T i - b\theta'$$

$$=> i = \frac{J\theta'' + b\theta'}{K_T}$$

Equation 21: Substituting Equation 8 into Equation 6

$$v_{in} = iR + K_b\theta'$$

Equation 22: Substituting Equation 9 into Equation 10 then Rearranging for θ``.

$$v_{in} = (\frac{J\theta'' + b\theta'}{K_T})R + K_b\theta'$$

$$=> K_T v_{in} = JR\theta'' + bR\theta' + K_T K_b\theta'$$

$$=> K_T v_{in} = JR\theta'' + (bR + K_T K_b)\theta'$$

$$=> K_T v_{in} - (bR + K_T K_b)\theta' = JR\theta''$$

$$\theta'' = \left(\frac{K_T}{JR}\right) v_{in} - (\frac{b}{J} + \frac{K_T K_b}{JR})\theta'$$

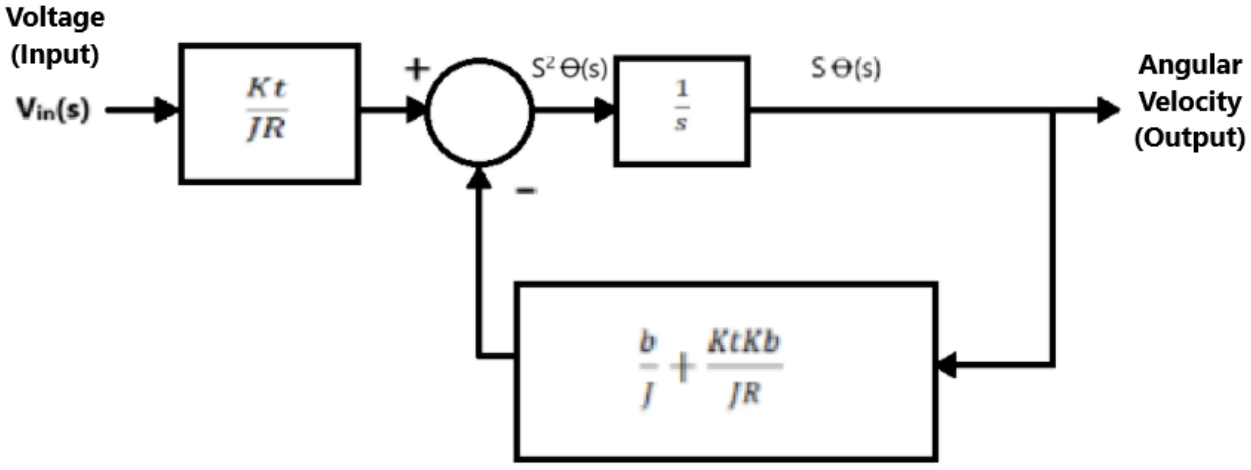

Figure 7: Motor Algebraic Block Diagram

Equation 23: Taking the Laplace Transform of Equation 11 and Rearranging for the Transfer Function

$$L\{\frac{d^2\theta(t)}{dt^2} = \left(\frac{K_T}{JR}\right)v_{in}(t) - (\frac{b}{J} + \frac{K_T K_b}{JR})\frac{d\theta(t)}{dt}\}$$

$$=> \ s^2\theta(s) = \left(\frac{K_T}{JR}\right)v_{in}(s) - (\frac{b}{J} + \frac{K_T K_b}{JR})s\theta(s)$$

$$=> \ s^2\theta(s) + (\frac{b}{J} + \frac{K_T K_b}{JR})s\theta(s) = \left(\frac{K_T}{JR}\right)v_{in}(s)$$

$$=> \left(s + \frac{b}{J} + \frac{K_T K_b}{JR}\right)s\theta(s) = \left(\frac{K_T}{JR}\right)v_{in}(s)$$

$$=> \frac{s\theta(s)}{v_{in}(s)} = \frac{\left(\frac{K_T}{JR}\right)}{\left(s + \frac{b}{J} + \frac{K_T K_b}{JR}\right)}$$

$$=> \frac{s\theta(s)}{v_{in}(s)} = \frac{K_T}{JRs + (bR + K_T K_b)}$$

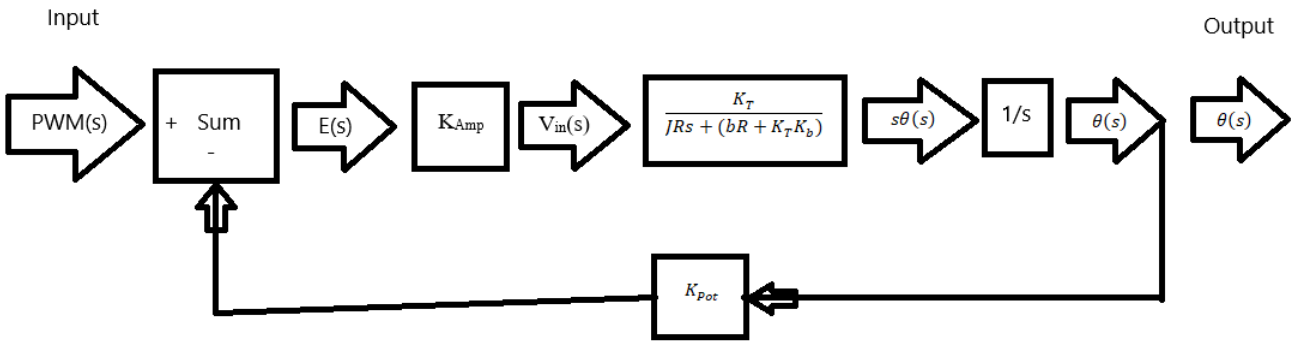

Figure 8: Servo Algebraic Block Diagram

Figure 8: Servo Algebraic Block Diagram shows the feedback control loop for the servo. The PWM signal is the input, K_{Amp} is the gain of the voltage amplifier, the transfer function for the DC motor (Equation 23) has been substituted in, K_{Pot} is the gain of the potentiometer, and the angular position(θ) is the output.

Table 3: DC Servo Algebraic Terms

Symbol	Description	SI Unit(s)
PWM(s)	Pulse Width Modulated signal (System input)	V (Volts)
θ(s)	Angular position of servo shaft (System output)	rad (Radians)
K_{Amp}	Voltage Amplifier gain	None (Constant)
K_{Pot}	Potentiometer gain	None (Constant)
For other terms refer to Table 2.		

Equation 24: Servo Transfer Function

$$\frac{\theta(s)}{PWM(s)} = \frac{\frac{K_{Amp}K_T}{JRs^2 + (bR + K_TK_b)s}}{1 + (\frac{K_{Amp}K_T}{JRs^2 + (bR + K_TK_b)s})(K_{Pot})}$$

$$=> \frac{\theta(s)}{PWM(s)} = \frac{K_{Amp}K_T}{JRs^2 + (bR + K_TK_b)s + (K_{Amp}K_TK_{Pot})}$$

From Equation 24, the transfer function describes a second order system as s^2 is the highest power of s in the denominator. The steady state gain of the system (when s=0) is equal to $(K_{Amp}K_T)/(K_{Amp}K_TK_{Pot})$. Assuming an ideal sensor $K_{Pot}=1$, thus the steady state gain is equal to one. This means at steady state the system output should be equal to the system input.

3.1.4 PID Controller

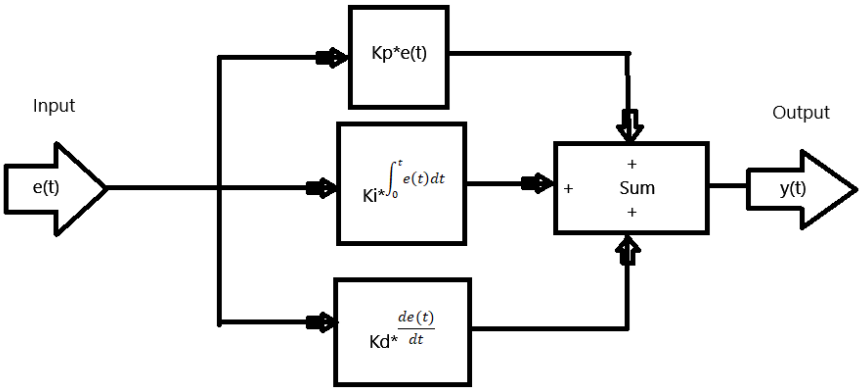

Figure 9: PID Controller Block Diagram

We can express PID control mathematically with the following equation. P, I, and D are represented by the three terms that add together here. K_p, K_i, and K_d are constants that tune how the system reacts to each factor.

e(t) is simply the instantaneous error at a point in time—the actual value of a controlled device minus the desired value. Multiply this by K_p and you have its contribution to the overall controller output.

The second term in this equation has to do with the combined error over time. It's the sum of all errors experienced on the device: Each time a controller calculates u(t), it adds the instantaneous error to a running tally. This figure is then multiplied by K_i and added into u(t).

The third term in this equation has to do with how fast the error changes.

Table 4: PID Algebraic Terms

Symbol	Description
y(t)	Controlled Output based on error. (output)
e(t)	System error. (input)
K_p	Error proportional gain.
K_i	Error integral gain.
K_d	Error derivative gain.

Equation 25: PID Differential Equation

$$y(t) = K_p e(t) + K_i \int_0^t e(t)dt + K_d \frac{de(t)}{dt}$$

Equation 26: Laplace Transform of Equation 14, Rearranged into the Transfer Function

$$L\{\, y(t) = K_p e(t) + K_i \int_0^t e(t)dt + K_d \frac{de(t)}{dt} \}$$

$$=>\ Y(s) = K_p E(s) + \frac{K_i}{s} E(s) + K_d s E(s)$$

$$=> \ Y(s) = (K_p + \frac{K_i}{s} + K_d s)E(s)$$

$$=> \ \frac{Y(s)}{E(s)} = \frac{K_d s^2 + K_p s + K_i}{s}$$

From Equation 26 it can be surmised that the PID controller is a first order system as there is an 's^{1}' term in the denominator.

3.1.5 Full System Control loop

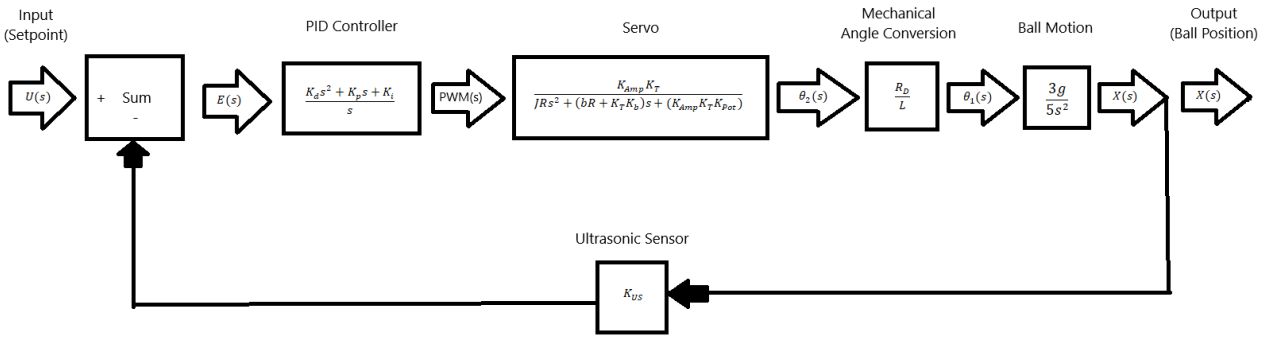

Figure 10: Full System Control Loop

Figure 10: Full System Control Loop shows the full system feedback loop. The input U(s) is the setpoint for the ball position and the output X(s) is the ball position as measured by the ultrasonic sensor.

Equation 27: Full System Transfer Function

$$\frac{X(s)}{U(s)} = \frac{G}{1 + GH}$$

$$=> \frac{X(s)}{U(s)}$$

$$= \frac{\left(\frac{K_d s^2 + K_p s + K_i}{s}\right)\left(\frac{K_{Amp}K_T}{JRs^2 + (bR + K_T K_b)s + \left(K_{Amp}K_T K_{Pot}\right)}\right)\left(\frac{R_D}{L}\right)\left(\frac{3g}{5s^2}\right)}{1 + \left(\left(\frac{K_d s^2 + K_p s + K_i}{s}\right)\left(\frac{K_{Amp}K_T}{JRs^2 + (bR + K_T K_b)s + \left(K_{Amp}K_T K_{Pot}\right)}\right)\left(\frac{R_D}{L}\right)\left(\frac{3g}{5s^2}\right)\right)(K_{US})}$$

$$=> \frac{X(s)}{U(s)}$$

$$= \frac{\left(K_d s^2 + K_p s + K_i\right)\left(K_{Amp}K_T\right)(R_D)(3g)}{(s)(JRs^2 + (bR + K_T K_b)s + \left(K_{Amp}K_T K_{Pot}\right))(L)(5s^2) + \left(\left(K_d s^2 + K_p s + K_i\right)\left(K_{Amp}K_T\right)(R_D)(3g)(K_{US})\right)}$$

$$=> \frac{X(s)}{U(s)}$$

$$= \frac{\left(K_d s^2 + K_p s + K_i\right)\left(3gK_{Amp}K_T R_D\right)}{\left(JRs^2 + (bR + K_T K_b)s + \left(K_{Amp}K_T K_{Pot}\right)\right)(5Ls^2)s + \left(K_d s^2 + K_p s + K_i\right)(3gK_{Amp}K_T K_{US}R_D)}$$

$$=> \frac{X(s)}{U(s)}$$

$$= \frac{\left(3gK_{Amp}K_s K_T R_D\right)s^2 + \left(3gK_{Amp}K_p K_T R_D\right)s + 3gK_{Amp}K_i K_T R_D}{(5JLR)s^5 + (5bLR + 5K_T K_b L)s^4 + \left(5K_{Amp}K_T K_{Pot}L\right)s^3 + \left(K_d s^2 + K_p s + K_i\right)(3gK_{Amp}K_T K_{US}R_D)}$$

From Equation 27, the transfer function is a fifth order system as there in an s^5 as the highest power of s in the denominator. (Note excluding the PID controller the system is fourth order) The steady

state gain of the system (when s=0) evaluates to $1/K_{US}$, assuming an ideal sensor means $K_{US}=1$. Thus, the system steady state output should be equal to the system setpoint.

3.1.6 System Simulation

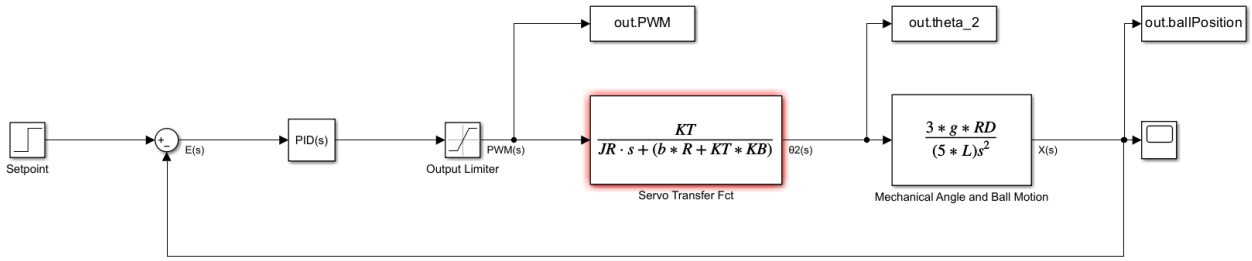

Figure 11: Full System Model [5]

Figure 11 shows the full system control loop implementation in Simulink. We were unable to use this model due to an inability to evaluate all the parameters of the servo transfer function. The servo (TowerPro MG995 Digi Hi-Speed) datasheet [21] is rather light on details, with no listed stall current being the biggest sticking point. Without one it isn't possible to find a value for the torque constant K_T or back emf constant K_b. The other challenging parameter to evaluate was the friction constant (b), given the servo's limited range of motion most experimental methods are unsuitable or risk damage. While we could assume b to be negligible, without K_T it isn't possible to make any progress with this model as a simulation of the built system configuration.

3.2 Ethical Considerations

Throughout the project ethics played an important role in the organisation of teamwork, consideration towards building materials and the execution of the work done. The team aimed to ensure that the following considerations were accounted for while maintaining progress on our project, resulting in an environmentally conscious and ethically built robot.

Work Distribution and Ethical Teamwork,

Teamwork describes a process in which a group of individuals work together towards a common goal [16]. To work effectively as a team, it is vital that the key components of teamwork ethics are respected by all members of the team. These areas include communication, respect, accountability and collaboration [17].

Communication and collaboration within the team ensures minimal conflict and a clear understanding between individuals while respect and accountability requires members to be aware of the opinions and actions of both themselves and those around them. To facilitate such co-operation, it was vital that workload be shared evenly and fairly amongst the team members, with respect to everyone's abilities. An example of such in this project was the allocation of sub teams to allow processes to develop simultaneously without overloading any individual group or person.

It is important that no individual is left feeling 'lost' due to neglect of responsibility by others or poor management of tasks. It is also important to respect the need to reprimand such misdemeanours and hold each other accountable to the responsibilities agreed. By practicing ethical teamwork, it allows for a higher standard of work through better problem solving, innovation and lower risks of burnout amongst individuals [18].

Health and Safety,

When working on the physical construction of the robot several health and safety related concerns surfaced surrounding the use of electrical components along with sharps and tools. Due to the nature of the electrical components and the need to utilise them, the risk of electrocution was ever present. The main risks surrounding electrical circuit are, but not limited to, electric shock and fire hazard.

Electric shock results from direct contact with live or faulty wires, which often leads to severe injuries or even in some cases death. Fire hazard is present in the form of short-circuiting wires connected to a power source or overloading of circuits due to improper wiring practices [19].

During the completion of the physical build, it was necessary to use potentially dangerous tools such as blades, screwdrivers and loose screws. In the use of any of these items there is a constant risk of unintentional harm to either oneself or others. As such it is crucial to use caution when handling such

tools and never complete tasks alone that you do not feel competent in. In the event an accident occurs, it is necessary to ensure that all group members understand the necessity of reporting injuries to a responsible party and how and where to find help if needed.

Environmental Impact

When approaching any project, environmental impact poses a significant challenge towards people across all disciplines. Specifically, when dealing with this project, the following concerns are relevant: sustainable use of materials, sustainable use of resources, energy consumption and proper disposal of electric components.

The material of choice for the balance beam construction needed to be easily modifiable as well as having minimal carbon footprint. To comply, many of the materials utilised in our build were either recycled or repurposed for their use, with the final robot being constructed from a mix of cardboard, scrap plywood and a galvanized strap for the stand.

Resources can be distributed sustainably through identifying areas of waste production and minimising any unnecessary need to replace functional components. Energy consumption is controlled through the reduction of unnecessary power use and only connecting power supplies for simulation purposes and disconnecting when not in use.

The disposal of electronics poses significant hazards toward both environmental health and human health through a combination of landfilling/ open dumping and open burning [20]. Such practices can result in the release of toxic chemical fumes into the air and harmful toxins and heavy metals into water sources as well as the surrounding earth [20]. The college aims to prevent this by providing Makeblock Ultimate 2.0 kits with the expectation that students will return them upon the completion of their projects.

4 IMPLEMENTATION & RESULTS

4.1 Physical System Build

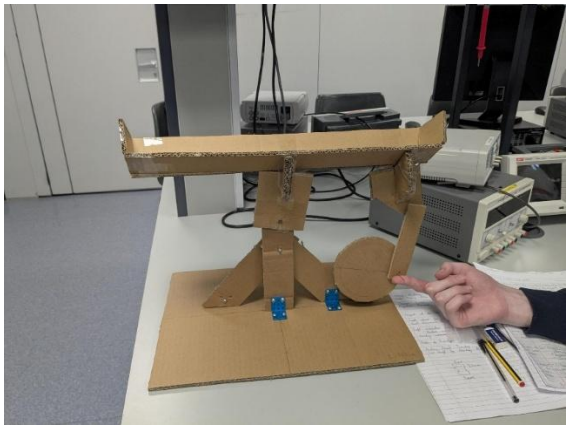

Figure 12: Cardboard Mock-Up of Mechanical Linkages

A cardboard mock-up of the system (Figure 12) was created to examine the physical linkages and identify any potential points where the mechanical system could collide with itself and break. The main insight gained from this initial examination was that increasing the radius to the connection point on the disk yielded a greater change to the angle of the main beam. Indicating a trade-off between the precision of the beam angle, and the maximum achievable angle plus the speed at which the angle could change.

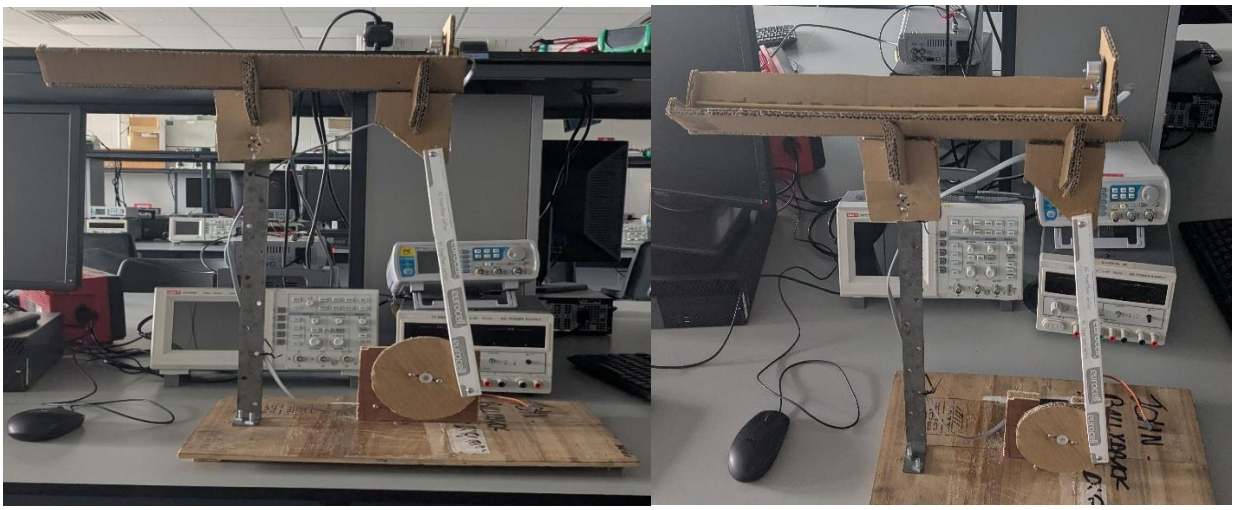

Figure 13: Physical System Build

Next a prototype was built using scrap materials including plywood, steel strapping and plastic. The upper cardboard channel was retained from the mockup to minimize weight acting against the motor. Care was taken to ensure that the perpendicular distance between the base of the channel and P_1 was equal to the perpendicular distance between the base of the channel and P_4. In doing so, the channel angle will be equal to the angle of the line between P_1 and P_4 and the horizontal axis. Taking the

wooden surface to the immediate left of the vertical steel upright as the origin point. The system measurement can be seen in Table 5.

Table 5: Built System measurements

Symbol	Description	Measurement
P_1	Location of bearing centre of rotation relative to origin.	(1.4 cm, 39.75 cm)
L	Distance between P_1 and P_4.	19.6 cm
P_3	Moving point at the centre of rotation about which C and L rotate.	
C	Distance between P_4 and P_3	33.15 cm
P_4	Moving point at the centre of rotation about which C and R rotate.	
R_D	Distance between P_2 and P_3	4.9 cm
P_2	Location of motor shaft centre of rotation relative to origin.	(21 cm, 7 cm)

4.2 Determining the linear range of motion

Using the values from table 5, the three equations (Eq. 13-15) from section 3.1.2 were plotted (Figure 14 below) with a range from -60° to +60°. The partially linear approximation (Equation 14) is quite accurate within [-30°,30°] as compared to the true equation (Equation 13). The fully linear approximation (Equation 15) is reasonably accurate within [-20°,40°]. Based on this, linearizing about the point (0°, 0°) if the system can operate within [-20°, 20°] the fully linearized approximation should be sufficiently accurate to model the system.

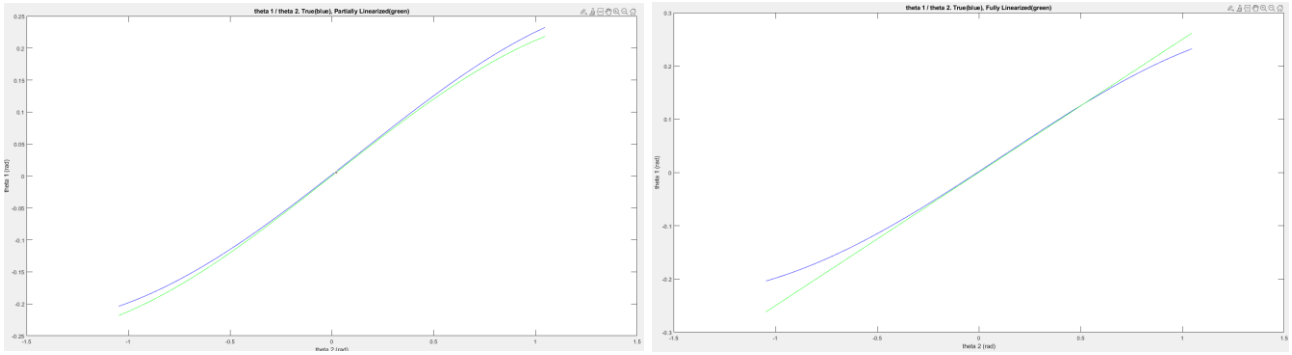

Figure 14: Plots Comparing the True Mechanical Relationship (blue) vs the Partially Linear Approximation (left) and vs the Fully Linear Approximation (right)

4.3 Torque on the motor disk due to the beam assembly weight

Part Name	Location (x,y) (cm)	Mass (grams)
Stopper Plate	(-21.6, 11.05)	0.86 g
Main Beam	(0, 10.05)	34.5 g
Bearing Connector 1 (lower)	(0, 2.58)	10.16 g
Bearing Connector 2 (upper)	(0, 6.54)	5.0 g
Rod Connector Plate 1 (lower)	(17.94, 3.46)	7.98 g
Rod Connector Plate 2 (upper)	(18, 7.01)	5.28 g
Sensor Plate	(20.9, 13.61)	22.0 g
Full Beam Assembly	**(7.92, 9.08)**	**85.78 g**

*All measurements are listed relative to the bearing's centre of rotation point (P1 discussed previously), when θ_1=0.

Combining all the above masses using the formula (Equation 28) yields the centre of mass of the full beam assembly.

Equation 28: Combined Centre of Mass of Multiple Masses for a Single Dimension [11]

$$C_x = \frac{x_1 m_1 + x_2 m_2 + \cdots + x_n m_n}{m_1 + m_2 + \cdots + m_n}$$

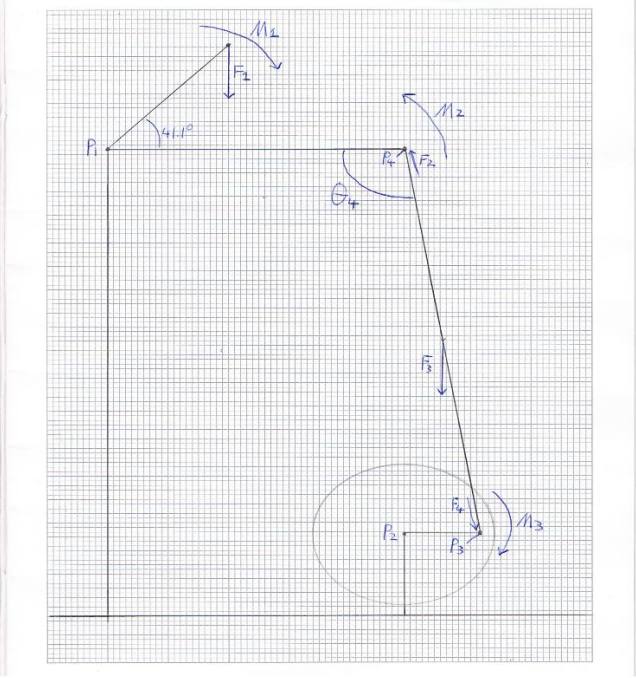

Figure 15: Free body diagram of weight forces and resultant moments. (θ_1, θ_2 = 0)

The moment forces (M_1 and M_2 above) acting on the top beam measured in N*cm, created by the weight force (F_1) and connecting rod (F_2) can be expressed generally as the following equations. (Within ±30°, unverified for larger angles.)

Equation 29: Moment of Bearing Caused by Weight Force (For θ_1 refer to Eq. 13)

$$M_1 = \sqrt{7.92^2 + 9.08^2} * (-9.81)(85.78 * 10^{-3})\sin(41.1° - \theta_1)$$

Equation 30: Moment of Bearing Caused by Connector Rod

$$M_2 = 19.6 * |F_2| * \sin(180° - \theta_4)$$

Equation 31: θ_4 using the cosine rule

$$c^2 = a^2 + b^2 - 2abcos(C)$$

$$=> C = \arccos\left(\frac{a^2 + b^2 - c^2}{2ab}\right)$$

$$\therefore \theta_4 = \arccos\left(\frac{19.6^2 + 33.15^2 - \left(\sqrt{(P_{1x} - P_{3x})^2 + (P_{1y} - P_{3y})^2}\right)^2}{2 * 19.6 * 33.15}\right)$$

$$=> \theta_4$$

$$= \arccos\left(\frac{19.6^2 + 33.15^2 - ((1.4 - (21 + 4.9\cos(\theta_2)))^2 + (39.95 - (7 + 4.9\sin(\theta_2)))^2)}{2 * 19.6 * 33.15}\right)$$

Equation 32: Moment Balance Equation, Rearranged for M_2

$$M_1 + M_2 = 0$$

$$=> M_2 = -M_1$$

Equation 33: Substituting Eq. 29, 30 into Eq. 32, then rearranging for $|F_2|$.

$$19.6 * |F_2| * \sin(180° - \theta_4) = -(\sqrt{7.92^2 + 9.08^2} * (-9.81)(85.78 * 10^{-3})\sin(41.1° - \theta_1))$$

$$=> |F_2| = -\frac{\sqrt{7.92^2 + 9.08^2} * (-9.81)(85.78 * 10^{-3})\sin(41.1° - \theta_1)}{19.6 * \sin(180° - \theta_4)}$$

To convert $|F_2|$ to its vector form pushing down along the beam, the angle between the connector rod and the horizontal axis needs to be found. This can be done by taking the arctan of the slope between points P_3 and P_4. See Equation 34 below.

Equation 34: Angle Between Connector Rod and the Horizontal Axis

$$\theta_{rod} = \arctan\left(\frac{P_{4y} - P_{3y}}{P_{4x} - P_{3x}}\right)$$

$$=> \theta_{rod} = \arctan\left(\frac{(39.75 + 19.6\sin(\theta_1)) - (7 + 4.9\sin(\theta_2))}{(1.4 + 19.6\cos(\theta_1)) - (21 + 4.9\cos(\theta_2))}\right)$$

Equation 35: F_2 in Vector Form

$$F_2 = [|F_2|\cos(\theta_{rod}), |F_2|\sin(\theta_{rod}), 0]$$

Equation 36: F_4 in vector form.

$$F_4 = F_2 + F_3$$

$$F_4 = \left[|F_2|\cos(\theta_{rod}), |F_2|\sin(\theta_{rod}) + (-9.81 * (29 * 10^{-3})), 0\right]$$

Equation 37: Position vector r (line from P_2 to P_3)

$$r = [4.9\cos(\theta_2), 4.9\sin(\theta_2), 0]$$

Equation 38: Moment of motor shaft due to weight force.

$$M_3 = r \times F = [0, 0, k]$$

Graphing the moment force exerted on the motor shaft by the weight force between [-30°, 30°] yielded Figure 17: Simplified system model below. The peak moment of -3.07 Ncm occurs when $\theta_2 \approx$ -5°, note a negative value denotes clockwise motion. The maximum moment output of the servo (TowerPro MG995 Digi Hi-Speed) is 83.36 Ncm, given that the peak weight moment value is <3.7% of the servo's, it will have a minimal effect on the system and won't be included in the simulation model.

In a larger scale engineering project this calculation would be required to determine the size of servo required to actuate the system without burning out or spending excessively on an overpowered servo.

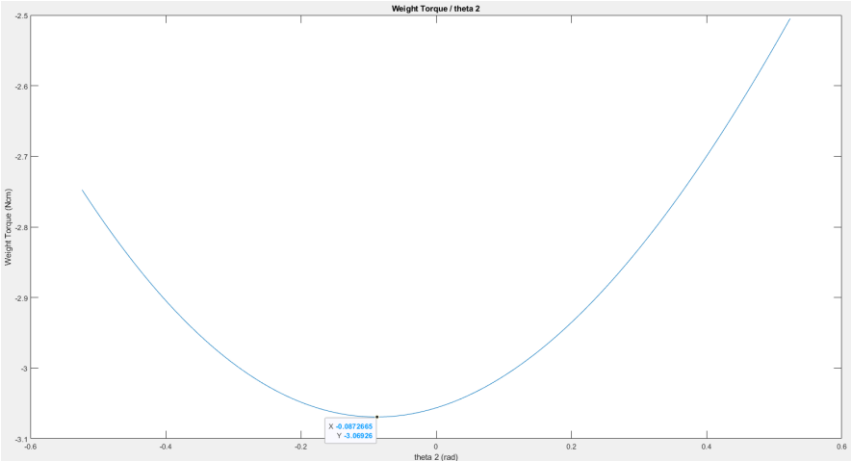

Figure 16: Plot of the Moment of the Motor Shaft Generated by the Weight Force of the Beam Assembly

4.4 Simulation Results

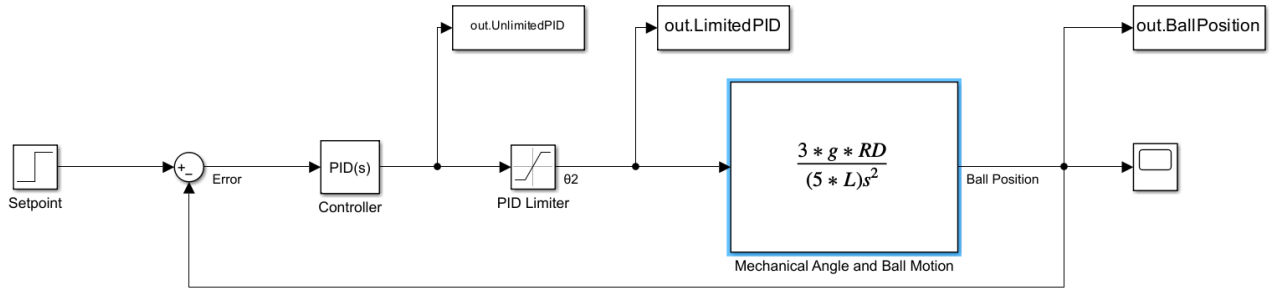

Figure 17: Simplified system model

Gathered from the library browser [5], these are the items used in Fig 12 (order from left to right):

- Step - To generate the step input signal, test how system reacts to change in input.
- Sum Block – By changing the sign that takes in the feedback loop to negative, this stabilizes and regulates the system which reduces error over time bringing the system to a steady state.
- PID controller – To achieve precise control over a dynamic system using its components Proportional (P), Integral (I) and Derivative (D) to calculate the control signal.
- Saturation Block – Limits the output of the PID controller within an upper and lower bound.
- Transfer Function Block- Computes the systems output for any given input by taking in the functions coefficients (numerator and denominator).
- Feedback loop (Not in library browser) - to take the feedback from the PID and transfer function and subtracting it from the desired outpoint in the sum block to calculate the error signal
- Scope- To visualise the behaviour of a system in graphical representation.

By assuming the servo can instantaneously achieve its steady state output, then its transfer function can be excluded, and the system can be simplified. Making this assumption invalidates this model's tuning values for use in the real system but affords the team a learning opportunity to experiment with tuning a PID controller for a marginally stable second order system.

Table 6: Model Parameters

Symbol	Description	Value (Unit(s))
g	Gravity value	981 cm/s^2
R_D	Distance from motor shaft(P_2) to push rod connection point on disk (P_3).	4.9 cm

L	Distance from bearing centre of rotation (P_1) to beam connection with push rod (P_4).	19.6cm

Applying a unit step input with just a K_p=1 value results in a continuously oscillating graph, as expected for a marginally stable system (Fig 18). Observing the PID output shows that the simulated servo position is outside of the range for which the model was deemed accurate back in section 4.2. To alleviate this a saturation block was added to keep the PID output within our determined limits.

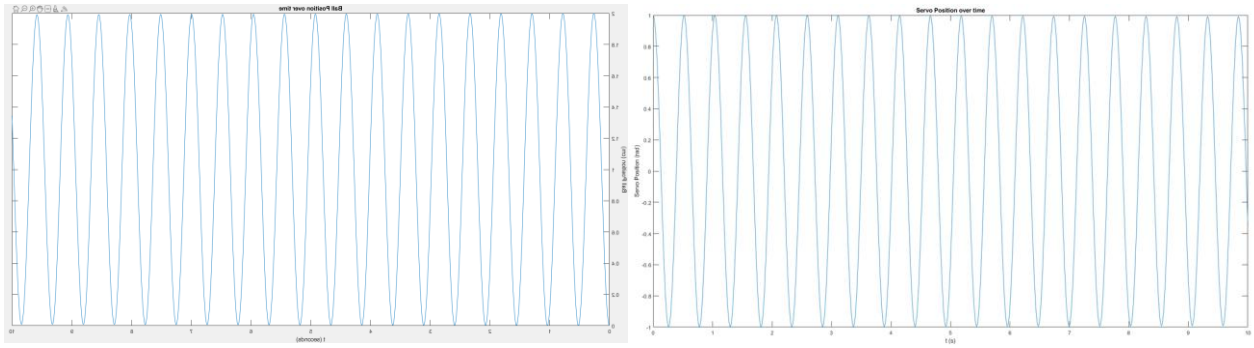

Figure 18: Ball Postion(left), Servo Position(right) both over time.

Rerunning the simulation with the saturation block in place with limits (-0.349 and 0.349) yielded figure 19. The square top on the servo graph shows the saturation block capping the value to keep it within range. This also causes the balls position to oscillate at a slower rate.

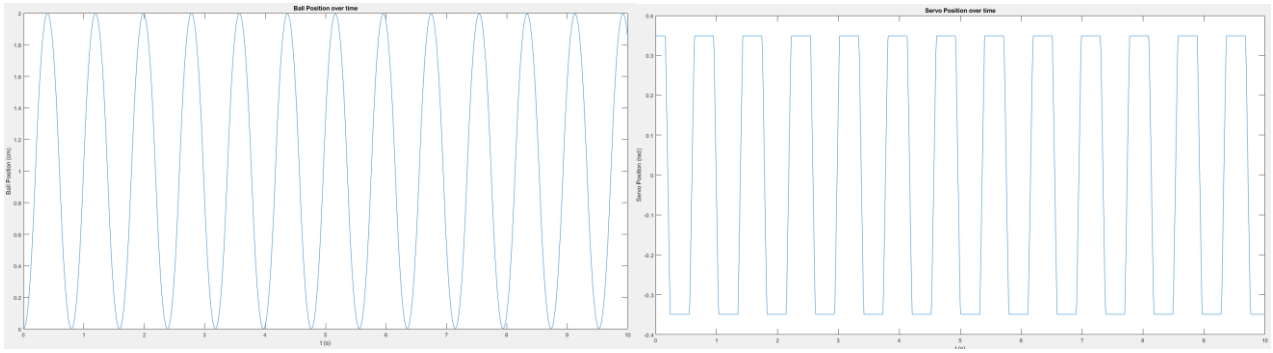

Figure 19: System simulation with limited PID output. Ball position(left), Servo position(right)

From here we attempted to apply the Ziegler-Nichols method to the system to tune the PID controller. This posed an unforeseen challenge as this system is always marginally stable for any value for K_p. To work around this, given that our system set point for the physical system well be 22 cm we selected a value for K_p that would saturate outside of a quarter beam length either side of the setpoint (Figure 20) e(t)=11, y(t)=0.349.

Equation 39: K_p Value

$$E(s) * K_p = Y(s)$$

$$K_p = \frac{0.349}{11} = 0.03172$$

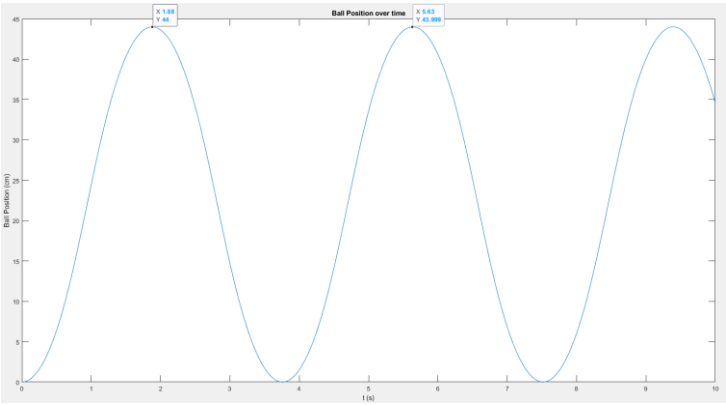

Figure 20: System response with setpoint=22 and K_p=0.03172

From Figure 20 we can measure the peak-to-peak time difference to determine the time constant (Tc=3.75s). Taking the applied K_p as our critical gain K_c. Appling the Ziegler-Nichols method leads to the following values. (Eq. 40-42)

Equation 40: Proportional gain

$$K_p = K_c * 0.6 = 0.019032$$

Equation 41: Integral gain

$$K_i = \frac{K_c}{(\frac{T_c}{2})} = \frac{0.03172}{(\frac{3.75}{2})} = 0.0169173$$

Equation 42: Derivative gain

$$K_d = K_c * \left(\frac{T_c}{8}\right) = 0.03172 * \left(\frac{3.75}{8}\right) = 0.014869$$

Simulating the system with the calculated values yields Figure 21. From it we can see the rise time of the system is 0.77 seconds, the peak overshoot is approximately 59.5%, and the settling time with a 5% tolerance band is 8.03 seconds. The system is also clearly underdamped so through an iterative process of slowly increasing K_d and decreasing K_i the system response was improved (Figure 22).

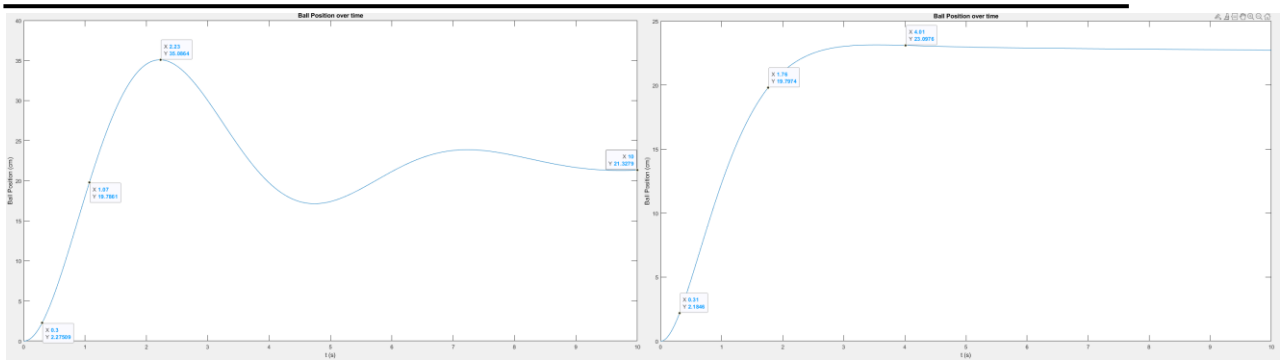

Figure 21a, b: System simulation with Ziegler-Nichols gain values(left). Refined gains(right)

The values used in figure 21b were: K_p=0.019032, K_i=0.0009, K_d=0.019. The K_i value has been reduced to less than 5% of the initial value while the K_d value has only been increased by 28%. The refined tuning values yield a rise time of 1.45 seconds, peak overshoot of 7% and settling time of 4.01 seconds. Based on this the team explored only using a PD controller for comparison (Figure 22).

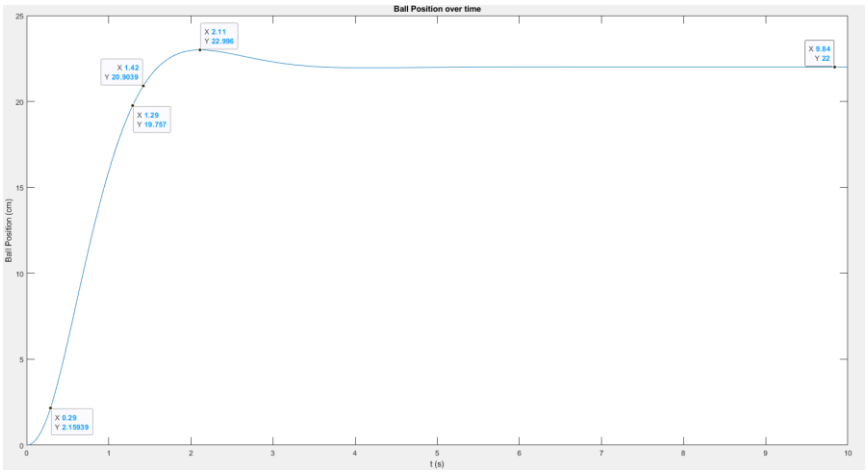

Figure 22: PD Controller system response

The PD controller achieved a significantly better result than the PID controller with values K_p=0.031 and K_d=0.02. These values yielded a rise time of 1 second, a peak overshoot of 4.5% and a settling time of 1.42 seconds. The team was satisfied with these results and hoped to be able to replicate them with the physical system.

4.5 DC Servo Motor and Ultrasonic Sensor

How the ultrasonic sensor and servo motor work:

We initially planned to use a stepper motor, but after running into issues with the control board and inconsistent movement, we switched to a Tower Pro MG995 servo motor. This servo turned out to be a solid replacement because it's easier to control and gives smoother, more precise angle adjustments. It works using a PWM (pulse-width modulation) signal; by sending a signal with a certain duty cycle, the servo moves to the corresponding angle between 0° and 180°. Internally, it has a potentiometer for feedback, which lets it check if it's at the right angle and correct itself if it's not. This feedback mechanism worked well with our PID controller, allowing the beam to respond smoothly to any changes in the ball's position. The MG995 also provides a decent amount of torque, so we didn't have any issues with it stalling or being too slow to react. Overall, it made the control system much more stable and reliable than what we were getting with the stepper motor.

The ultrasonic sensor complements this by continuously measuring the distance to the ball. It works by emitting high-frequency sound waves and timing the echo's return. This timing helps calculate how far the ball is, providing the data needed to adjust the beam's angle.

Testing our Sensor and Motor:

We tested our servo and ultrasonic sensor to ensure that both worked. We tested them by connecting tree wires to its own terminal each and inputted its terminals into C++ code for the servo and block code for our sensor. We used our USB A-B cable to install our code onto the Arduino micro-controller. We finally attached two wires to the positive and negative terminals and saw that our motor and sensor worked.

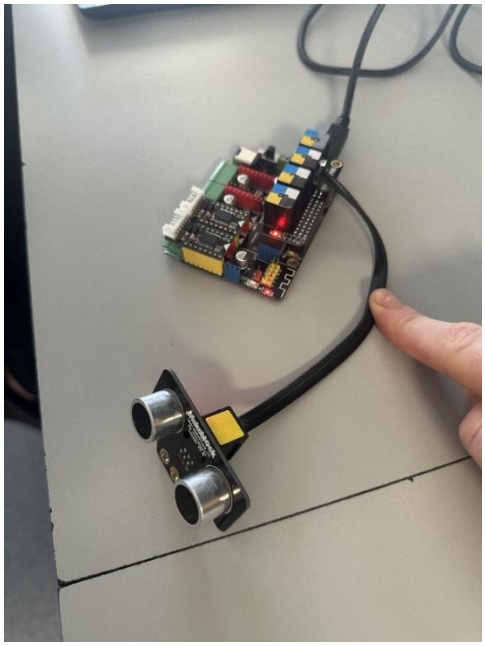

Figure 24: Ultrasonic Sensor

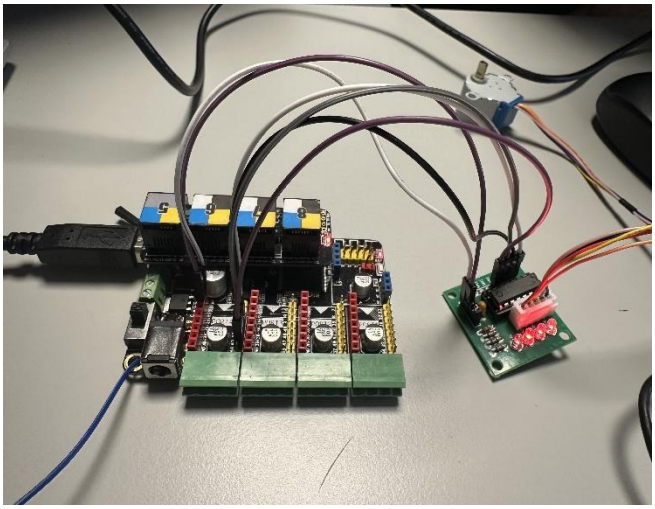

Figure 23: Arduino & Stepper Motor Boards

Problems we encountered with the equipment

Applying the components above to the physical model we assembled the project however during installation we ran into numerous hardware problems.

The first problem of many which we quickly identified was with the stepper motor, the problem we had was that it spun clockwise but wouldn't spin anticlockwise we quickly came to realise this issue and switched it out for the servo motor which we used for the remainder of the project.

The main problem we encountered was with the ultrasonic sensor where it would read an incorrect distance of 40cm (length of beam) which meant that at between 6-6.5cm (max range of 20) in the beam the waves were able to bypass the ball and progress to the end of the beam and back. This was a problem as it created a large error signal which then caused an erratic jerk movement in the beam that disrupted the control loop not allowing it to settle the balls position.

To solve this problem, we tried mounting the sensor in many different positions and orientations to try get the ultrasonic sound waves to transmit to and bounce back from the ball in a consistent manner.

The issue persisted, so we tried a larger ball (8cm) with the hope enlarging the surface area would improve detection. This unfortunately also didn't work; a new issue was identified this time when the ball was close to the sensor, we noticed that it picked up the distance about 2cm in from the ball's edge. When that same ball was at the far end of beam it would read closer to 6cm in from the ball's edge. Returning to the ping-pong ball (4cm) we also observed this inconsistent measurement point. This was very confusing so our last try to resolve this issue was to adjust the code.

Our final attempt to resolve this issue after weeks of troubleshooting was to try and take an average of 2 previous readings, and if a new reading was 4cm above or below the average it would ignore that reading and take another. This filtering method also failed to eliminate the erroneous readings.

Due to time constraints, it was decided to reallocate our time to refining the mathematical model and simulation results due to there being no guarantee that the hardware issues wouldn't persistent.

5 CONCLUSIONS & FURTHER WORK

In conclusion, this project has significantly sharpened each team member's communication, mathematical reasoning, and control-systems expertise. The process of working through the technical details of the project as a team gave everyone valuable insight into the real-life applications of the theory covered throughout both the first year BEng and BSci courses. Although a single inadequate component prevented us from fully realizing the prototype, we refined our time-management processes and gained invaluable, hands-on experience building and visualizing our feedback loop in MATLAB. The resulting closed-loop response graphs not only validated our theoretical models but also pinpointed exactly where to focus our next effort laying the groundwork for a robust, fully functional design in the future.

Further works could involve investigating alternative designs for the physical build, such as having the table rolling inside of an enclosing tube, which would eliminate the inaccurate sensor readings that occurred due to outside interference. Such interferences could include, but are not limited to; noise interference, the round thin surface of the ball scattering the tracking sound wave, which are all a result of the nature of ultrasonic sensors. It is also important to note that if reapproaching such a project again it would be important to consider alternative distance sensors, notably infrared or time of flight which perform better when measuring complex 3-dimensional surfaces as well as producing higher accuracy readings due to having higher reading frequencies [22].

6 REFERENCES

[1] Dr. P. Bhousule, G. Chiou, A. Plascencia and T. Rowe "Balancing a ball and beam with PID", Dept. of Elec. Eng., Univ. of Texas at San Antonio, RAM Lab, TX, USA, 2016

[2] OpenStax, "11.3: Dynamics of Rotational Motion – Rotational Inertia", *Physics Libretexts*, 2024. [Online]. Available: https://phys.libretexts.org/Bookshelves/College_Physics/College_Physics_1e_(OpenStax)/10%3A_Rotational_Motion_and_Angular_Momentum/10.03%3A_Dynamics_of_Rotational_Motion_-_Rotational_Inertia. [Accessed: Feb. 25, 2025]

[3] OpenStax, "11.2: Rolling Motion", Physics *LibreTexts,* 2024. [Online]. Available: https://phys.libretexts.org/Bookshelves/University_Physics/University_Physics_(OpenStax)/Book%3A_University_Physics_I_Mechanics_Sound_Oscillations_and_Waves_(OpenStax)/11%3A__Angular_Momentum/11.02%3A_Rolling_Motion. [Accessed: Feb. 25, 2025]

[4] Lectures by Walter Lewin. *8.01x - Lect 24 - Rolling Motion, Gyroscopes, VERY NON-INTUITIVE*. (Feb. 8, 2015). Accessed: Mar. 4, 2025. [Online Video]. Available: https://www.youtube.com/watch?v=XPUuF_dECVI [Accessed: Feb. 28, 2025]

[5] The MathsWork Inc., "Block Libraries", *Simulink Documentation,* 2024[Online]. Available: https://uk.mathworks.com/help/simulink/block-libraries.html. [Accessed: Mar. 11, 2025]

[6] G. Zhen, S. Wijesinghe, T. Pathinathanpillai, E. Dyer and I. Singh 'Design and Implementation a Ball Balancing System for Control Theory Course', IJMEC, Universal Scientific Org., www.aeuso.org, Sept 10, 2015 – Available: Vol5_Iss17_2363_2374_Design_and_Implementation_a_Ball_Ba.pdf

[7] P. Bhandari and P. Z Csurcsia "Ball Balancing Beam Design of a PID-controller", VRIJE Univ. Brussels, Mar 29, 2021, Available: manual_v1.pdf

[8] S. McLoone (2024). EE114 Introduction to Systems and Control [PowerPoint Slides]. Available: https://moodle.maynoothuniversity.ie/course/view.php?id=37786 [Accessed: Feb – May 2025]

[9] P. Dawkins, "Laplace Transform Table", Paul's Online Notes, 2024. [Online]. Available: https://tutorial.math.lamar.edu/classes/de/laplace_table.aspx. [Accessed: Mar. 4, 2025]

[10] The MathsWorks Inc., "Transfer Functions," MATLAB & *Simulink Documentation*, 2024. [Online]. Available: https://uk.mathworks.com/help/control/ug/transfer-functions.html. [Accessed: Mar. 4, 2025]

[11] T.Weideman, "System with Multiple Particles", Univ. of California, Davis, Physics Libre Texts [Online] Available: 4.2: Center of Mass - Physics LibreTexts [Accessed: Apr. 20, 2025]

[12] Image Source: https://ctms.engin.umich.edu/CTMS/index.php?example=MotorSpeed&section=SystemModeling

[13] Matt Bilsky, "ME207 DC Motor Model Equation Derivation" (Feb. 3, 2017) [Online Video] Available: ME207 DC Motor Model Equation Derivation - YouTube [Accessed: Apr. 22, 2025]

[14] DMD Engineering "How to Model a DC Motor as a System of ODEs" (Jul. 28. 2020) [Online Video] Available: How to Model a DC Motor as a System of ODEs [Accessed: Apr. 22, 2025]

[15] True Geometry "Calculating Air Resistance using the Drag Equation in Context of How to Calculate Air Resistance" [Online Blog] Available: Calculating air resistance using the drag equation in context of how to calculate air resistance | True Geometry's Blog [Accessed, Mar. 11, 2025]

[16] E. Perry "What will make or break your next role? Find out why teamwork matters", BetterUp.com [Online Blog] Apr. 7, 2022, Available: What Is Teamwork and Why Does It Matter? [Accessed May. 6, 2025]

[17] SkillMaker Admin "The Importance of Teamwork Ethics in the Workplace" [Online Blog] Nov. 2024 Available: The Importance of Teamwork Ethics in the Workplace - Skillmaker [Accessed: May. 06, 2025]

[18] T. Middleton "The importance of teamwork (as proven by science)", atlassian.com [Online Blog] Jan. 25, 2024, Available: What is teamwork and why is it important? - Work Life by Atlassian [Accessed: May. 06, 2025]

[19] R. Ogle “Safety First: Essential Electronics Safety Tips for Beginners”, electroviz.com [Online Blog] Aug. 30, 2023, Available: Safety First: Essential Electronics Safety Tips for Beginners [Accessed: May. 07, 2025]

[20] S. Devika, "Environmental impact of improper disposal of electronic waste," *Recent Advances in Space Technology Services and Climate Change 2010 (RSTS & CC-2010)*, Chennai, India, 2010, pp. 29-31, doi: 10.1109/RSTSCC.2010.5712793, Available: Environmental impact of improper disposal of electronic waste | IEEE Conference Publication | IEEE Xplore [Accessed: May. 07, 2025]

[21] Unknown , “MG995 High Speed Metal Gear Dual Ball Bearing Servo”, soldered.com [Online Data Sheet] Available: MG995 - Tower-Pro [Accessed: Mar. 25, 2025]

[22] ‘Shawn’, “Types of Distance Sensors and How to Select One”, 2020, [Online] Available: Types of Distance Sensors and How to Select One? - Latest News from Seeed Studio [Accessed: Mar. 29, 2025]